Accurate control of ion bombardment in remote plasmas using pulse-shaped biasing

Accurate control of ion bombardment in remote plasmas using pulse-shaped biasing

P. Kudlacek,[a] R. F. Rumphorst, and M. C. M. van de Sanden
Department of Applied Physics, Plasma and Material Processing Group, Eindhoven University of Technology, 5600 MB Eindhoven, The Netherlands

(Received 29 June 2009; accepted 17 August 2009; published online 7 October 2009)

This paper deals with a pulsed biasing technique employed to a downstream expanding thermal plasma. Two pulsed biasing approaches are presented: asymmetric rectangular pulses and modulated pulses with a linear voltage slope during the pulse, and their applicability is discussed on the basis of the intrinsic capacitance of the processed substrate-layer system. The substrate voltage and current waveforms are measured, and the relation to the obtained ion energy distributions is discussed. Accurate control of the ion bombardment is demonstrated for both aforementioned cases, and the cause of broadening of the peaks in the ion energy spectra is determined as well. Moreover, several methods to determine the modulated pulse duration, such that the sloping voltage exactly compensates for the drop of the substrate sheath potential due to charging, are presented and their accuracy is discussed. © *2009 American Institute of Physics*. [doi:10.1063/1.3225690]

I. INTRODUCTION

Remote plasmas are extensively used in industry for both etching and deposition of materials. In both cases an additional bias voltage is often applied to the substrate to control the energy of the bombarding ions and/or enlarge their flux onto the substrate. Ion bombardment has been demonstrated to be crucial for controlling material properties[1] or enhancing etch rate and anisotropy during ion induced etching.[2] For conductive substrates, a dc bias can be employed and ions bombard the substrate with a well-defined energy. However, when insulating substrates are being processed, charge is quickly build up on the surface, reducing the flux and energy of bombarding ions. To remedy this "surface charging effect," a radio frequency (rf) bias is typically used, but its capability to control the energy of the bombarding ions is limited for physical reasons. The ion sheath transit time is usually shorter than the rf period, and ions respond to the instantaneous sheath voltage. Thus, their final energies depend strongly on the phase of the rf cycle in which they enter the sheath, resulting in a bimodal ion energy distribution (IED).[3,4] Although increasing the frequency seems to be the way of narrowing the IED,[5] this approach suffers from the following limitations. The width of IED becomes significantly mass dependent for high bias frequencies, and as a result the IED remains bimodal for low mass ions often produced in processing plasmas. Moreover, at frequencies where the rf wavelength is comparable to the substrate dimensions, voltage nonuniformities across the substrate surface can be induced,[6] leading to process nonuniformities.

Recently, a pulsed bias scheme became subject of increased interest as a promising technique to reach narrow, almost monoenergetic IED when a dielectric substrate is being processed. In addition it offers an ultimate control of the ion flux onto the substrate by varying the duty cycle (defined as the ratio of pulse duration to the total period of the pulse). Earlier literature refers to an asymmetric rectangular pulsed bias, where the charging effect is minimized by shortening the pulse duration.[7–9] Nevertheless, for a few microseconds lasting pulses, a displacement current, naturally present after the pulse start and end, becomes a limiting factor because it physically limits the possibility of the substrate voltage and current control.[8] To overcome these limitations, Wang and Wendt[10] introduced a modulated pulsed approach, where the voltage during the pulse is sloped and thus exactly compensates for the drop of voltage due to the charging of the substrate being processed.

This paper focuses on two cases of using pulsed biasing which are dramatically different due to an intrinsic capacitance of the substrate-thin film system. Each of them benefits from one of the aforementioned pulsed bias approaches. The intrinsic capacitance is defined as $C_i=\varepsilon_0\varepsilon_r/d$, where ε_0, ε_r, and d are the permittivity of free space, the relative permittivity, and the insulator thickness, respectively. When an insulator, exposed to the plasma from one side and biased from the other, is treated as two parallel plates of a planar capacitor, a simple equation for the voltage drop across the dielectric due to the charging can be derived:

$$dV/dt = J_s/C_i, \tag{1}$$

where J_s stands for the substrate current density. Note that the charging effect has been similarly treated for rf cycles in Ref. 11 and for asymmetric pulses in Ref. 7.

To illustrate the first case, let us assume a deposition of 1 μm of SiO_2 film on a c-Si wafer using an expanding thermal plasma (ETP) (discussed hereafter) with a substrate current density of $J_s=1$ mA/cm^2. In this worst case scenario (J_s is during the deposition realistically about ten times lower and the deposited layer is usually thinner than 1 μm) Eq. (1) leads to a voltage drop at the substrate surface of 3 V within 10 μs pulse duration. In this example, the drop of voltage does not need to be compensated because during the whole

[a]Electronic mail: p.kudlacek@tue.nl.

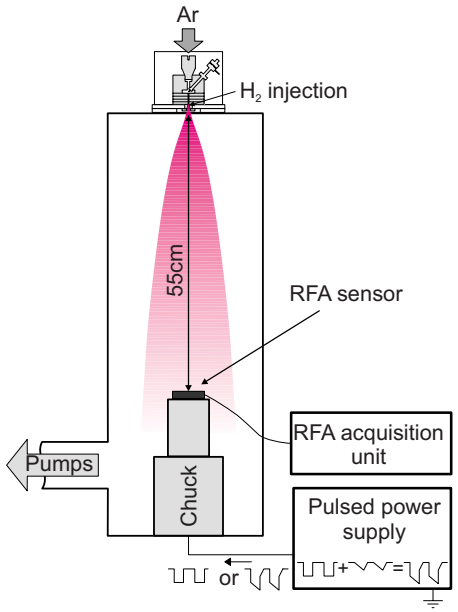

FIG. 1. (Color online) Schematic picture of the experimental setup.

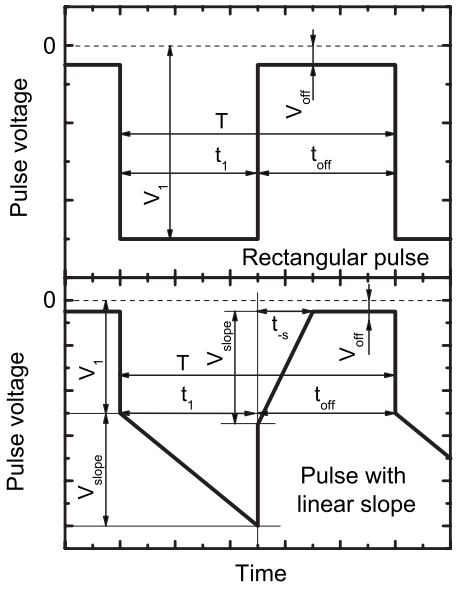

FIG. 2. Dimensioned pulse shapes. T is the pulse period, t_1 is the pulse duration, t_{off} is the off pulse duration, t_{-s} is the duration of the negative linear slope, V_1 is the pulse voltage, V_{off} is the voltage during the off pulse, and V_{slope} is the maximum of the linear slope.

10 μs pulse, the substrate sheath potential, the primary factor that determines the distribution of ions bombarding the substrate, would be sufficiently stationary, resulting in an IED that would be adequately narrow. Therefore, in this case rectangular asymmetric pulses can still be used. Whereupon the second case, the deposition of a material on a standard glass substrate 0.5 mm thick, under the conditions mentioned above, one gets a severe charging effect. Equation (1) leads to a voltage drop of 150 V within a 1 μs pulse duration, which is too high and even for shorter pulses the voltage during the pulse should be increased in order to keep the substrate sheath potential constant. Otherwise, without sloping of the bias voltage, the substrate sheath potential would linearly decrease in time, resulting in a broad IED.

Recently, the pulsed bias has been successfully employed to an ETP to enhance deposited film properties[12–14] and ion induced etching.[15] Several theoretical studies on pulsed biasing published so far present mostly IEDs modeled on the basis of mentioned model [Eq. (1)] (Ref. 8) or on the sheath voltage measurement.[10] The directly measured IEDs for asymmetric rectangular pulses have been published by Barnat and Lu.[9] This paper reports on measurements using a retarding field energy analyzer (RFEA) to characterize the ion bombardment on pulse biased substrates. A direct measurement of the IED was not possible when the ion bombardment on a dielectric substrate was studied, and therefore only modeled IEDs, based on accurate substrate voltage and current measurement, are presented and discussed.

II. EXPERIMENTAL DETAILS

All experiments were performed in an ETP reactor which is duly described in Refs. 16 and 17 and schematically depicted in Fig. 1. Briefly, the plasma is generated by an argon-fed subatmospheric pressure cascaded arc and then supersonically expands into a low pressure (10–100 Pa) deposition chamber. Hydrogen is injected directly into the cascaded arc's nozzle, resulting in a cooling and quenching of emanating argon plasma mainly through $Ar^+ + H_2$ collisions.[18] More details on chemistry and transporting phenomena in the Ar/H_2 expanding plasmas can be found in Ref. 19. During experiments, 50 standard cubic centimeters per second (sccs) of argon flow and 2 sccs of hydrogen were employed, and the pressure in the deposition chamber was kept constant at 18 Pa.

A homemade pulsed power supply capable to operate in a frequency range of 1–210 kHz was directly coupled to a chuck on which a substrate holder or the RFEA was clamped. The pulsed power supply generates rectangular asymmetric pulses with variable voltage level during on pulse, $V_1 = -10$ to -300 V, and during off pulse, $V_{off} = -12$ to +5 V, and can deliver dc and peak current up to 200 mA and ~2 A, respectively. Pulse duration t_1, as well as an off pulse duration t_{off}, is variable from ~2.3 to ~500 μs. As an option, the mentioned rectangular pulses can be combined with triangular pulses, i.e., the voltage during the pulse operation is sloped (see Fig. 2). The maximum of the voltage drop during the sloped pulse is fixed to $V_{slope} = 100$ V, and the duration of a negative slope after the pulse end is variable in two steps, $t_{-s} = 2$ and 20 μs. Available shapes of the pulse with dimensioned quantities are depicted in Fig. 2. Note that this pulsed power supply has been designed in house with respect to industrial requirements as a more cost-effective and more robust substitute for the usually used waveform generator and broadband amplifier.[10,12–15]

The substrate current I_s and substrate voltage V_s were simultaneously measured by means of a Tektronix TCP312 current probe and a Tektronix 1/100 passive voltage probe, respectively. An extra wire loop, required for substrate current measurement and used to feed the bias voltage to the substrate as well (see Fig. 3), was found to have a high impedance for the frequencies of interest (10–200 kHz). Moreover, it unacceptably limits the frequency bandwidth for the substrate voltage measurements. Therefore, a setup

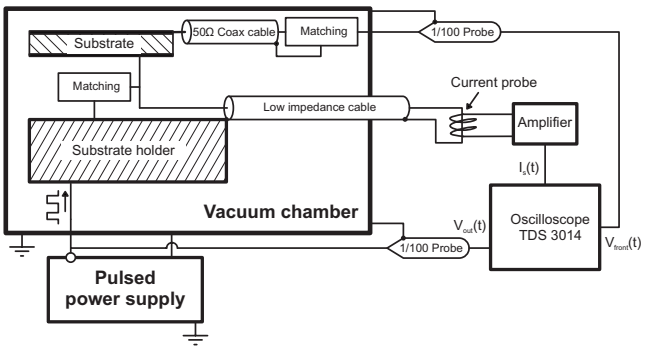

FIG. 3. Schematic picture of the setup for the measurement of the applied pulse voltage V_{out}, the substrate surface voltage V_{front}, and the substrate current I_s.

(schematically depicted in Fig. 3), with matching circuits incorporated in the substrate holder, has been implemented in order to make simultaneous monitoring of both the substrate current and the substrate voltage possible. The achieved correspondence of the pulsed power supply output voltage V_{out} with the measured substrate voltage V_s is better than 97% within the frequency bandwidth of up to 30 MHz.

Two types of dummy substrates were used: a tungsten plate of 25 cm^2 and a, on both sides, gold plated alumina substrate of 6.45 cm^2, 0.5 mm thick with a capacitance of 166 pF to mimic a conductive and a dielectric substrate, respectively. Figure 3 shows the setup with the mounted dielectric dummy substrate when, in contrast with the conductive substrate, an additional voltage at the substrate surface, V_{front}, was measured. Due to the mentioned equality of V_{out} with V_s, waveforms for I_s, V_s (V_{out}), and V_{front} could be simultaneously measured even when a dielectric substrate is used.

The commercial planar gridded RFEA (Semion system[20]) was used to measure time-averaged energy distributions of ions bombarding the pulse biased substrate, placed at a distance of 55 cm from the arc nozzle from which the plasma emanates. The sensor, as well as an acquisition unit, has been customized in order to allow time-averaged measurement under low and mid frequencies of the pulsed bias voltage applied. A detailed description of RFEA principle can be found in Ref. 21. As the sensor is compact (0.6 mm thick) a pumping of the sensor is not needed under the pressure range of interest since the mean free path $\lambda = 2.8$ mm is greater than the distance traveled by the ions within the sensor. The mean free path was calculated for neutral-neutral momentum transfer collisions with the ideal gas approach using Sutherland's law (Ar, $p=18$ Pa, $T=500$ K) and is comparable to a mean free path measured under similar conditions and presented in Ref. 22. Moreover, the obtained ion energy distributions did not show artifacts, such as a significant fraction of ions with "negative" energy, expected when collisions within the sensor would play a significant role.

The electron temperature T_e and the ion density n_i were measured by means of a double Langmuir probe in the vicinity of the substrate in the center of the reactor. The theory described by Peterson and Talbot[23] was used to process the obtained I-V characteristics. An effective ion mass of 3 amu was used in the analysis related to the fact that the most abundant ion impinging the substrate under these conditions is H_3^+.[24]

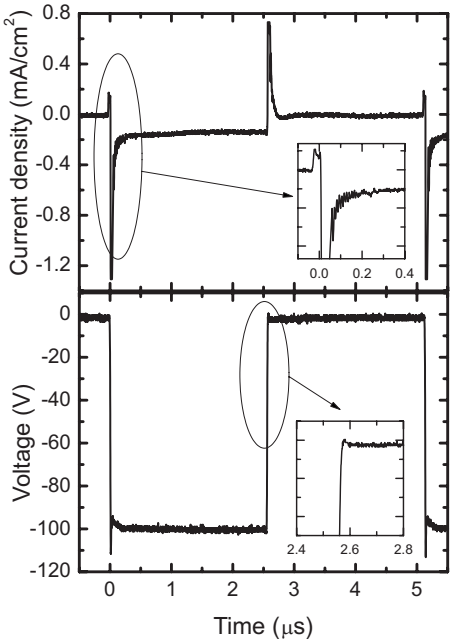

FIG. 4. Typical substrate current density J_s (top) and the substrate voltage V_s (bottom) waveforms measured on the conductive dummy substrate for the pulse voltage $V_1 = -100$ V, the pulsed frequency of 195 kHz, and the duty cycle of 50%.

III. RESULTS AND DISCUSSION

A. Substrate voltage and current waveforms

Figure 4 shows the typical substrate voltage V_s and the substrate current density J_s waveforms of a directly coupled asymmetric rectangular pulsed bias for a pulse voltage $V_1 = -100$ V, a pulsed frequency of 195 kHz, and a duty cycle of 50%. The voltage during the off pulse V_{off} was set in such a way that the resulting substrate current during the off pulse was zero, i.e., equal to the floating potential ($V_{off} \sim V_f = -2$ V). Waveforms for different frequencies are principally similar and hence, all further argumentation is applicable to them too.

The pulsing of the substrate potential causes an expected temporal independence of the substrate ion flux on the substrate voltage due to a displacement current. This independence is associated with the restructuring of the sheath at the beginning and at the end of the pulse to the steady-state conditions. When the pulse starts, the electrons are instantaneously repelled from the biased electrode, which leads to a temporal excess of ions within the sheath. These ions are drained to the electrode, resulting in a displacement current. When the sheath approaches equilibrium, the displacement current decays and the ion current is henceforth the steady-state conduction current (the so-called Bohm current). Likewise, when the electrode is pulsed back from a large negative potential to a lower value, the electrons instantaneously flow from the plasma into the sheath because of the reduced field across the sheath. Excess of electrons within the sheath tem-

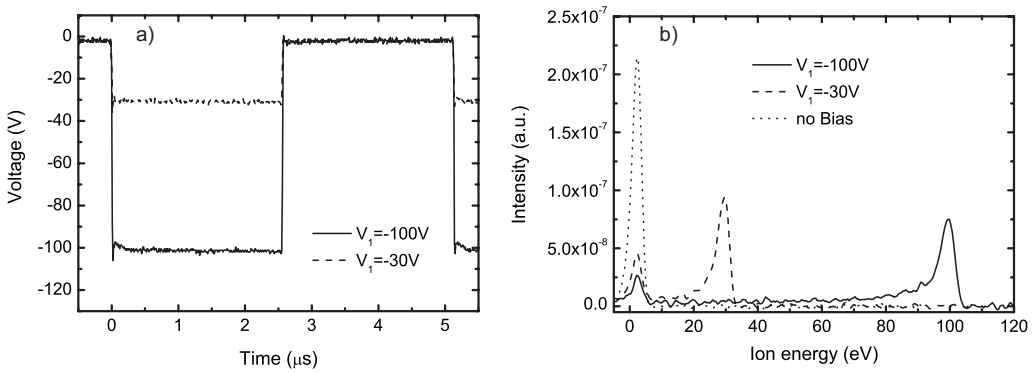

FIG. 5. Applied pulsed bias voltage waveforms (a) and the resulting time-averaged ion energy distributions (b) for the pulse frequency of 195 kHz, the duty cycle of 50%, and two various voltages during the pulse $V_1=-30$ (solid line) and -100 V (dashed line); IED measured on the unbiased electrode (dotted lines) is depicted for comparison.

porarily reduces the electrode current, and the ions have to "fill in" this region until equilibrium is again established, as has been modeled by Barnat and Lu.[8]

In order to quantitatively compare the measured displacement current with theory, it will be useful to define a time to establish the steady-state Child law sheath.[25] This time is approximately equal to

$$t_c \approx \frac{\sqrt{2}}{9}\omega_{pi}^{-1}\left(\frac{2V_0}{T_e}\right)^{3/4}. \quad (2)$$

Here, V_0 is the voltage variation of the electrode, $\omega_{pi}=\sqrt{(e^2n_0)/(\varepsilon_0 M)}$ is the ion plasma frequency, n_0 is the bulk ion plasma density, e is the elementary charge, ε_0 is the permittivity of free space, and M is the ion mass. Further, we assume that the rise time of the voltage pulse is significantly shorter than the time to establish the steady-state Child law sheath, t_c. As both the rise and fall times of the pulses are approximately 25 ns, this assumption is satisfied in the present case. Substituting the electron temperature of about 0.15 eV, bulk ion density of 2×10^{16} m^{-3} (measured by means of the double Langmuir probe), H_3^+ as the predominant ion, and a 100 V voltage drop, Eq. (2) leads to a sheath recovery time of ~300 ns, which is in good agreement with the decay time of the current peak measured after the pulse start (see Fig. 4). As can be seen in Fig. 4, the substrate current reaches a positive value right after the pulse ends, although only a drop of current would be expected according to the previous explanation. This feature is connected to an overshooting of the substrate voltage, visible after the pulse ends, to a positive value with respect to the floating potential (see Fig. 4). This means that due to the absence of a retarding field, electrons can freely move to the electrode and constitute the electron current until the ions establish the equilibrium.

B. Control of IED: Conductive substrate

As it has been mentioned, the rectangular asymmetric pulses can be used to bias a conductive substrate even when a dielectric layer is being deposited on it. The influence of the shape of the asymmetric rectangular pulse voltage on the energy of bombarding ions was measured, and the IEDs and the corresponding substrate voltage waveforms are depicted in Figs. 5–7.

Figure 5 shows the effect of pulse voltage variation $V_1=-30$ and -100 V for a pulse frequency of 195 kHz and a duty cycle of 50%. The voltage during the off pulse V_{off} was kept at the floating potential, i.e., $V_{\text{off}}\sim V_f=-2$ V. Energy distribution function of ions bombarding the unbiased electrode under the same ETP conditions is depicted for comparison. Generally, the distributions with two peaks are expected due to time averaging and alternating of the substrate voltage between two voltage levels. As the energy which ions gain due to the bias voltage V_b is equal to $e(V_p-V_b)$, where $V_p\approx0.2$ V is the plasma potential (estimated from the measured IEDs), the high energy and low energy peaks approxi-

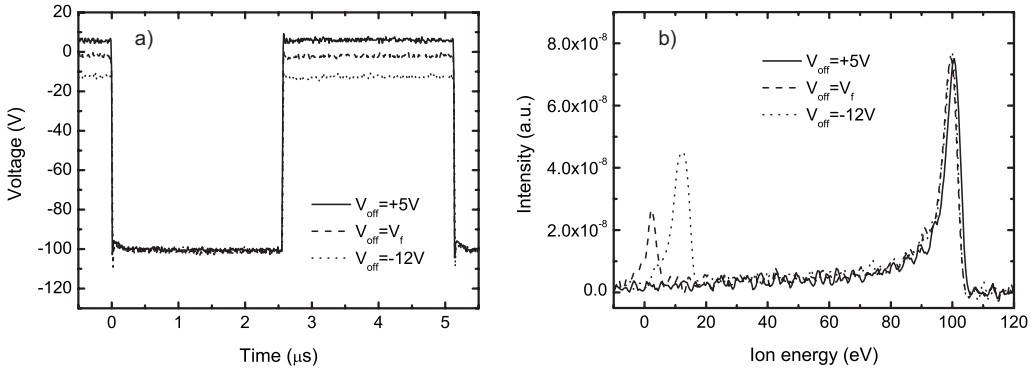

FIG. 6. Applied pulsed bias voltage waveforms (a) and the resulting time-averaged ion energy distributions (b) for the pulse frequency of 195 kHz, the voltage during a pulse of -100 V, the duty cycle of 50%, and various voltages during the off pulse $V_{\text{off}}=+5$ V (solid line), floating potential (dashed line), and -12 V (dotted line).

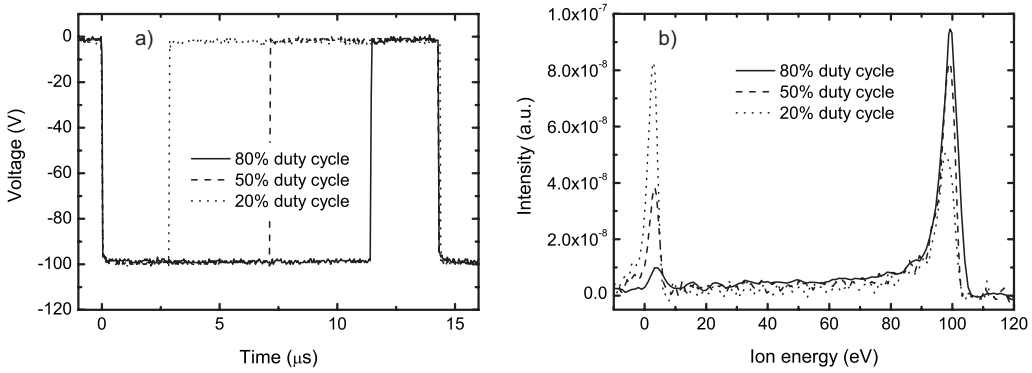

FIG. 7. Applied pulsed bias voltage waveforms (a) and the resulting time-averaged ion energy distributions (b) for the pulse frequency of 70 kHz, the voltage during the pulse of −100 V, and various duty cycles of 80% (solid line), 50% (dashed line), and 20% (dotted line).

mately match with the applied V_1 and the V_{off} voltages, respectively. The effect of V_{off} variation for the same pulsed frequency and duty cycle is shown in Fig. 6, and the correspondence of the V_{off} voltage with the position of low energy peak of the IEDs is obvious. The integral intensity of the low peaks is then given by the overall ion current, collected on the substrate during off pulse, which depends mainly on the difference between the floating potential and the applied V_{off} voltage. It is well known that the ion current as a function of electrode potential starts decaying exponentially in the vicinity of the floating potential as a result of increasing potential barrier for ions. Therefore, the integral intensity of low energy peaks decreases when the V_{off} increases and the peak even disappears for V_{off} markedly higher than the floating potential. It means that the ion flux is suppressed and the electron current is predominantly collected on the substrate, leading to the monoenergetic IED [see Fig. 6(b)]. It should be noted that V_{off} can be effectively used to control the substrate sheath potential during off pulse only in the situation when a conductive material is being processed. For insulating substrates the charge accumulated on the substrate surface during the pulse has to be discharged at the beginning of the off pulse after which the substrate sheath potential reaches the floating potential despite the V_{off} setting.

Figure 7 shows the time-averaged ion energy distributions obtained for the pulse voltage $V_1=-100$ V, a frequency of 70 kHz, and various duty cycles. The voltage during rest period, V_{off}, was again kept at the floating potential. As expected, the IED obtained for the 80% duty cycle approaches a monoenergetic distribution, while the low energy peak of the distribution measured for the 20% duty cycle is more pronounced than its high energy peak as a natural consequence of the time averaging during RFEA measurement. In principle similar ion energy spectra would be obtained for all frequencies of the pulsed power supply's frequency range. Only for long pulses the drop of potential across the dielectric due to its charging should be taken into account when a conductive substrate with dielectric layer is biased [see Eq. (1)].

1. Broadening of IED

There are several physical reasons causing a broadening of the ion energy distribution. The most important are the substrate sheath potential variation, thermalization of ions due to the collisions in the sheath, and last but not least the influence of the ion sheath transition time. Apart from this, the broadening as a consequence of the scattering of ions on the RFEA's grids or due to collisions within the sensor can play a role. As it has been noted above, the effect of collisions within the sensor is regarded as insignificant, and the predominant measurement error is given by the used five-point derivative method in calculating the IED curves from the measured collector current. Our estimation leads to a 2 eV broadening at full width at half maximum of the ion peaks as an artifact of the measurement, which is negligible with respect to the measured broadening. The sheath transition time of ions becomes important for higher frequencies[9] and hence, only the first two aforementioned physical reasons will be important for our discussion.

Except for the drop of substrate sheath voltage due to the charging which is discussed below, the substrate sheath potential can slightly vary in time mainly due to the applied pulsed voltage instabilities. These instabilities, which can cause peak broadening, are hardly visible from the voltage waveforms and therefore, to highlight their importance, it will be worth to use the measured substrate voltage and current waveforms to model the IEDs. Normalized ion energy distributions $N(\varepsilon)$, taking into account the measured substrate voltage $V_s(t)$, and the substrate ion current density $J_{is}(t)$ can be obtained by calculating normalized integrals over the whole pulsed period T of the filter function $F(t,\varepsilon)$ equal to $J_{is}(t)$ for ions possessing energies between $e[V_s(t)\pm\Delta V/2]$ and zero for the rest of energies:

$$F(t,\varepsilon)=\begin{cases} J_{is}(t) & \text{for } \varepsilon/e \in \langle V_s(t)\pm\Delta V/2\rangle \\ 0 & \text{for } \varepsilon/e \notin \langle V_s(t)\pm\Delta V/2\rangle \end{cases}, \tag{3}$$

then

$$N(\varepsilon)=\frac{\int_{\text{period}}F(t,\varepsilon)dt}{\int_{\text{period}}J_{is}(t)dt}. \tag{4}$$

The ion substrate current density J_{is} is then calculated from the measured substrate current density J_s using the Langmuir probe theory for a flat electrode:

$$J_{is}=J_s-J_e^*e^{-e(V_p-V_s)/kT_e} \quad \text{for } V_s<V_p, \tag{5}$$

where J_e^* is the saturated electron current density, $V_p \approx 0.2$ V is the plasma potential with respect to the ground potential, and k is the Boltzmann constant. The normalized

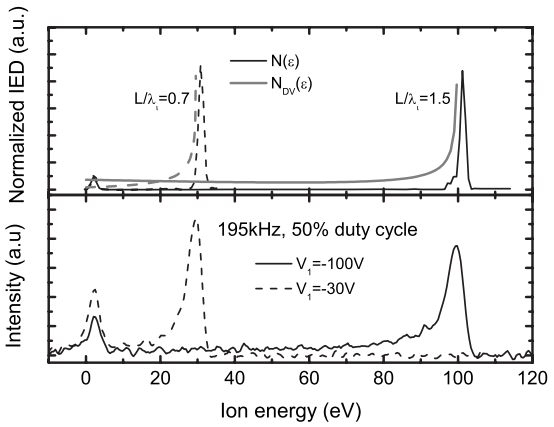

FIG. 8. Normalized ion energy distributions calculated on the basis of the Davis–Vanderslice's model $N_{DV}(\varepsilon)$ and on the basis of the measured substrate voltage and current waveforms $N(\varepsilon)$ (top) for the pulse frequency of 195 kHz, the duty cycle of 50%, and two various voltages during the pulse $V_1=-30$ (solid line) and -100 V (dashed line); ion energy distributions measured under the same conditions are depicted for comparison (bottom).

distributions $N(\varepsilon)$ calculated for a pulse frequency of 195 kHz, a duty cycle of 50%, and the pulse voltages $V_1=-30$ and -100 V are depicted in Fig. 8 (top) and show a good agreement with the measured IEDs [Fig. 8 (bottom)]. This approach can also be used as a reliable alternative for the experimentally measured IED when the measurement is difficult or if just an estimation of the shape of the IED suffices. The IED obtained for $V_1=-100$ V exhibits a slightly greater broadening of the high energy peak compared to the distribution measured under the same condition for $V_1=-30$ V [see Fig. 8 (bottom)]. The high energy peaks reveal a "shoulder," which suggests scattering losses of the ion energy due to collisions within the sheath. The model treating the broadening of the IED due to collisions in the sheath has been introduced by Davis and Vanderslice,[26] taking into account an average number of collisions that ions undergo within the sheath, L/λ_i, i.e., the sheath thickness divided by the ion mean free path. Considering the collisionless Child law sheath, the corresponding sheath thicknesses L are 1.95 (the measured steady-state substrate current density during the pulse $J_s^{st}=0.135$ mA/cm^2) and 4.16 mm ($J_s^{st}=0.18$ mA/cm^2) for pulse voltages of -30 and -100 V, respectively. Since $\lambda_i \approx \lambda = 2.8$ mm under the condition of interest, the ratio L/λ_i reaches approximately values of 0.7 and 1.5 for $V_1=-30$ and -100 V, respectively. Davis and Vanderslice's distribution is prescribed as a parametric function of L/λ_i as

$$N_{DV}(\varepsilon) = \frac{L}{\lambda_i}\left(\frac{1}{2\sqrt{1-\varepsilon/(eV_c)}}\right)e^{-(L/\lambda_i)[1-\sqrt{1-\varepsilon/(eV_c)}]}, \qquad (6)$$

where V_c is the voltage applied to the electrode with respect to the plasma potential (sheath voltage). Calculated distributions corresponding to $L/\lambda_i=0.7$ and 1.5 are depicted in Fig. 8 (top) and qualitatively reveal the influence of collisions on the peak broadening. Note that only fractions of 50% for $V_1=-30$ V and 22% for $V_1=-100$ V of the ions reach the electrode with the maximum energy and the rest constitutes the shoulder of the high energy peak of the distribution [see Fig. 8 (bottom)].

In comparing the modeled ion energy distributions $N(\varepsilon)$ and $N_{DV}(\varepsilon)$ with the experimentally measured IEDs, the predominance of broadening of the peaks due to collisions is obvious as well as that broadening caused by the small applied voltage variation is not negligible.

C. Control of IED: Dielectric substrate

It has been described that the use of a dielectric substrate leads to a fast drop of substrate sheath potential due to the charging. To demonstrate this, Fig. 9 shows simultaneously the behavior of the substrate current density J_s, the applied substrate bias voltage V_{out}, and the voltage measured at the substrate surface V_{front} for the rectangular pulses (left panel) and for the pulses with linear voltage slope (right panel). As the contribution of the plasma potential to the overall substrate sheath potential is negligible in our case ($V_p \approx 0.2$ V), V_{front} will be considered as the substrate sheath potential henceforth. We would like to emphasize that the substrate sheath potential V_{front} is the result of the capacitive coupling of V_{out} voltage through the dielectric substrate. Consequently, the substrate current collected over the whole period has to be equal to zero, and the substrate sheath potential during the off pulse reaches the floating potential after the accumulated charge is fully discharged, as it can be seen in Fig. 9.

When rectangular pulses are used, the dielectric substrate is being charged and consequently V_{front} decreases until it reaches the floating potential at a time t_z after the pulse starts [see Fig. 9(a)]. Considering that the drop of V_{front} obeys Eq. (1), understanding the behavior of J_s as a function of time and instantaneous substrate sheath potential [$J_s = J_s(t, V_{front})$] is crucial. After the start of the pulse, the displacement current charges the dielectric, causing a fast drop of the substrate sheath potential. Thereupon, the conductive substrate current governs the charging, and the drop of voltage obeys a mutual relation between the substrate current density J_s and the substrate sheath potential V_{front}. Assuming that J_s is a linear function of V_{front} for $V_{front} \ll V_f$, caused by the enlargement of the active area of the substrate with rising substrate sheath potential[27] (see also Fig. 2 in Ref. 7), Eq. (1) leads to a quadratic drop of V_{front} with time. V_{front} starts dropping more rapidly when it approaches the floating potential as the substrate current becomes affected by the electron current, and V_{front} lastly stabilizes at the floating potential.

When the voltage during the pulse is linearly sloped ($V_{slope}=100$ V) and the pulse duration t_1 is set in such a way that the slope exactly compensates for the drop of the substrate sheath potential caused by charging, V_{front} approaches a rectangular shape, as can be seen in Fig. 9(b). V_{front} during the pulse is not entirely flat due to both the displacement current and the aforementioned dependence of the substrate current on the substrate sheath voltage. Especially the displacement current leads to a fast substrate sheath potential drop, evident right after the pulse start, which is the main reason for the discrepancy between the value of V_{front} during the pulse with the preset pulse voltage V_1 (neglecting V_{off} as $V_{off} \approx V_f$), cf. Fig. 9(b), when $V_1=-100$ V and the resulting V_{front} during the pulse is ~ -80 V. After the end of the pulse,

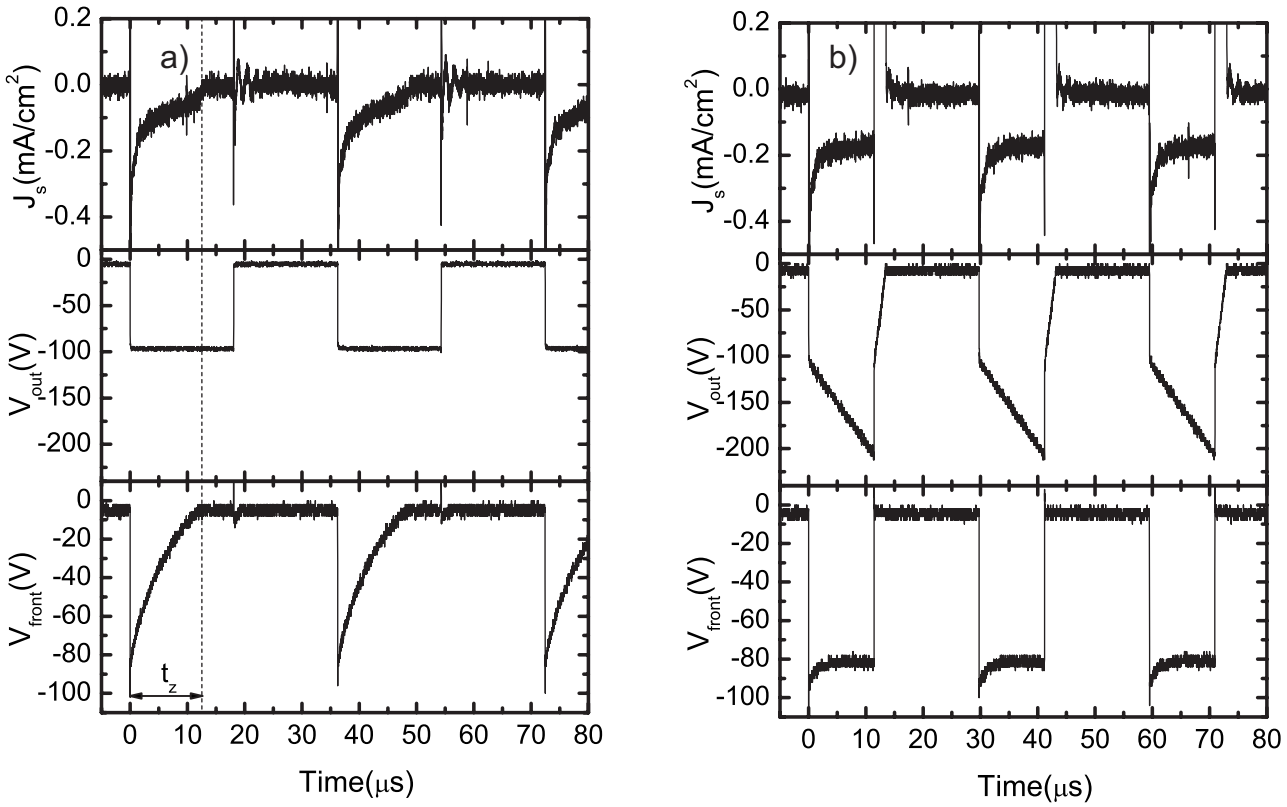

FIG. 9. The waveforms for the substrate current density J_s (top), the applied pulsed voltage V_{out} (middle), and the resulting substrate sheath voltage V_{front} (bottom) simultaneously measured on the dielectric dummy substrate for the rectangular pulses (a) and for the pulses with the linear slope (b).

the negative linear slope pulls the substrate sheath voltage to a slightly positive potential with respect to the floating potential, resulting in an electron current driven discharging of the accumulated charge. Potentially high values of the electron current can be lowered down by a slower negative sloping of the bias voltage, i.e., prolongation of t_{-s}, in the case that the exposure of the substrate to a high electron current might be unwanted due to the sensitivity of the processed material. Note that until the accumulated charge is fully discharged the electrons are predominantly collected on the substrate. Consequently, the ion energy distribution, when the next pulse starts right after the negative slope, will be monoenergetic, similar to the distribution depicted in Fig. 6(b) (solid line).

The modeled ion energy distributions for both presented cases of using dielectric substrate are depicted in Fig. 10. As expected, the fast drop of the substrate sheath potential when the rectangular pulses are used leads to a very broad IED, while the distribution for pulses containing a linear voltage slope clearly reveals a narrow distribution.

1. Estimation of the pulse duration

It is obvious from Secs. III B and III C that an accurate determination of t_z, the pulse duration leading to the rectangular waveform of V_{front}, is important to keep the energy of bombarding ions within narrow boundaries. Although the direct observation of the V_{front} behavior is the most accurate way of the t_z determination, such measurement can be experimentally difficult or even impossible, for instance, during the film deposition. Then other methods have to be used.

Experimental estimation of t_z can be done from the substrate current response to the rectangular pulse with the pulse voltage equal to the maximum of the voltage slope ($V_1 = V_{slope}$). Then t_z is the time for which the substrate current reaches zero [illustrated in Fig. 9(a)]. The advantage of this method is that it can be easily implemented into the dedicated pulsed power supply as a feedback, allowing the automatic control of the V_{front} voltage. Such a feature is useful when the intrinsic capacitance of the substrate significantly changes during its processing (deposition of a thick film or fast etching of a large area of the substrate). Knowing the substrate current density J_s and the intrinsic capacitance C_i, the duration of the pulse t_z can also be calculated from the following equation:

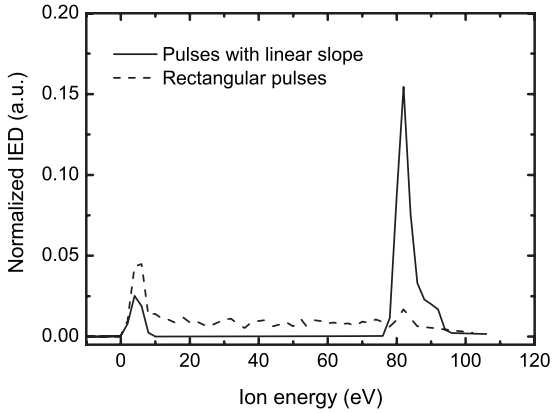

FIG. 10. The calculated (on the basis of the measured substrate voltage and current waveforms) energy distributions of ions bombarding the dielectric dummy substrate, pulse biased by the pulses with the linear slope (solid line) and by the rectangular pulses (dashed line).

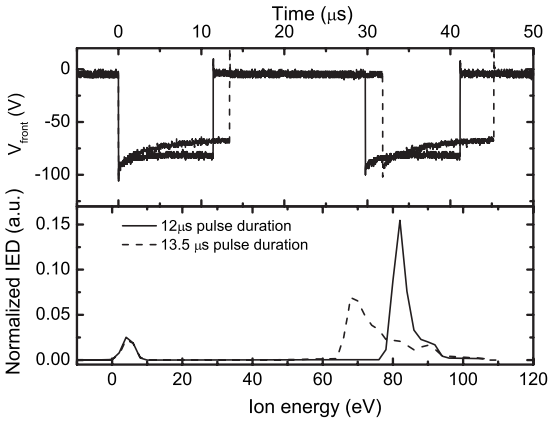

FIG. 11. The substrate sheath voltage waveforms (top) and the calculated (on the basis of the measured substrate voltage and current waveforms) energy distributions of ions bombarding the dielectric dummy substrate for two preset pulse durations (bottom).

$$\int_0^{t_z} J_s(t)|_{V_1} = \frac{C_i}{V_{\text{slope}}}, \tag{7}$$

assuming that the pulse starts at $t=0$.

The mentioned methods have been used to determine the pulse length t_z for the case of the previously used dielectric dummy substrate in order to assess their accuracy. The pulse length t_z determined from the current response is equal to 12.5 μs, use of Eq. (7) leading to a pulse duration of 12.2 μs, while the best value set manually according to the V_{front} shape was 12 μs (depicted in Fig. 9). Even considering the high sensitivity of the resulting V_{front} shape on the preset $t_1=t_z$, both mentioned methods lead to reasonably accurate results, i.e., the resulting IED will be narrow. It is worth mentioning that the calculation using Eq. (7) can be simplified for long pulses, where the overall contribution of the displacement current to the actual substrate current is negligible. Then a steady-state value of the substrate current density during the pulse $J_s^{\text{st}}|_{V_1}$ can be used instead of the integration of the $J_s(t)$. Such simplification leads to the pulse length of $t_z=13.5$ μs for the presented case, which is too inaccurate. V_{front} waveforms together with the resulting normalized ion energy distributions $N(\varepsilon)$ for pulse duration of $t_z=12$ and 13.5 μs are depicted in Fig. 11 to show distortion of the IED caused by inaccurate setting of the pulse duration t_z. Besides the obvious sensitivity of the IED shape on the preset pulse length, the results also highlight the importance of the accurate substrate current measurement, as it is essential for the proper determination of the t_z by any method.

IV. CONCLUSIONS

It has been shown that the pulsed biasing of a dielectric substrate and a conductive substrate with a dielectric layer on it has to be established by different pulsed biasing approaches due to their intrinsic capacitance. Asymmetric rectangular pulses suffice for the biasing of a conductive substrate with a dielectric layer on it, as the charging effect is not too significant. On the other hand, the modulated pulses with a voltage slope during the pulse should be used when a dielectric substrate is processed. A setup for simultaneous monitoring of the pulsed power supply output voltage, the substrate voltage, and the substrate current has been developed. Ion energy distributions are shown for both aforementioned cases in order to demonstrate capabilities of the dedicated power supply to manipulate the ion energy and their flux onto the substrate and discussed on the basis of the obtained substrate voltage and current waveforms. Ion energy spectra are also compared to Davis–Vanderslice's model in order to quantify the broadening of the peaks due to the collisions of ions within the sheath. Several methods to determine the modulated pulse duration, such that the sloping voltage exactly compensates for the drop of the substrate sheath potential due to charging, have been presented and their accuracy discussed.

ACKNOWLEDGMENTS

This work was in part supported by OTB-Solar.

[1] S. M. Rossnagel and J. J. Cuomo, Vacuum **38**, 73 (1988).
[2] C. C. Tin, T. H. Lin, and Y. Tzeng, J. Electrochem. Soc. **138**, 3094 (1991).
[3] Ch. Wild and P. Koidl, Appl. Phys. Lett. **54**, 505 (1989).
[4] E. Kawamura, V. Vahedi, M. A. Lieberman, and C. K. Birdsall, Plasma Sources Sci. Technol. **8**, R45 (1999).
[5] W. M. Holber and J. Forster, J. Vac. Sci. Technol. A **8**, 3720 (1990).
[6] J. E. Stevens, M. J. Sowa, and J. L. Cecchi, J. Vac. Sci. Technol. A **14**, 139 (1996).
[7] E. V. Barnat and T.-M. Lu, J. Vac. Sci. Technol. A **17**, 3322 (1999).
[8] E. V. Barnat and T.-M. Lu, Phys. Rev. E **66**, 056401 (2002).
[9] E. V. Barnat and T.-M. Lu, J. Appl. Phys. **92**, 2984 (2002).
[10] S.-B. Wang and A. E. Wendt, J. Appl. Phys. **88**, 643 (2000).
[11] B. Chapman, *Glow Discharge Processes: Sputtering and Plasma Etching* (Wiley-Interscience, New York, 1980), Chap. 5.
[12] I. Martin, M. A. Wank, M. A. Blauw, R. A. C. M. M. van Swaaij, W. M. M. Kessels, and M. C. M. van de Sanden, "The effect of low frequency pulse-shaped substrate bias on the remote plasma deposition of *a*-Si:H thin films," Plasma Sources Sci. Technol. (submitted).
[13] M. A. Blauw, M. Creatore, and M. C. M. van de Sanden, "Densification of silicon dioxide by energetic ion impact during plasma deposition" (unpublished).
[14] M. A. Wank, I. Martin, M. A. Blauw, R. A. C. M. M. van Swaaij, and M. C. M. van de Sanden, *Proceedings of the SAFE2006*, Veldhoven, The Netherlands (STW Technology Foundation, Utrecht, The Netherlands, 2006), p. 488.
[15] M. A. Blauw, P. J. W. van Lankvelt, F. Roozeboom, M. C. M. van de Sanden, and W. M. M. Kessels, Electrochem. Solid-State Lett. **10**, H309 (2007).
[16] M. C. M. van de Sanden, G. M. Janssen, J. M. de Regt, D. C. Schram, J. A. M. van der Mullen, and B. van der Sijde, Rev. Sci. Instrum. **63**, 3369 (1992).
[17] M. C. M. van de Sanden, R. J. Severens, W. M. M. Kessels, R. F. G. Meulenbroeks, and D. C. Schram, J. Appl. Phys. **84**, 2426 (1998).
[18] R. F. G. Meulenbroeks, A. J. van Beek, A. J. G. van Helvoort, M. C. M. van de Sanden, and D. C. Schram, Phys. Rev. E **49**, 4397 (1994).
[19] S. Mazouffre, M. G. H. Boogaarts, I. S. J. Bakker, P. Vankan, R. Engeln, and D. C. Schram, Phys. Rev. E **64**, 016411 (2001).
[20] www.impedans.com.
[21] D. Gahan, B. Dolinaj, and M. B. Hopkins, Rev. Sci. Instrum. **79**, 033502 (2008).
[22] R. Engeln, S. Mazouffre, P. Vankan, D. C. Schram, and N. Sadeghi, Plasma Sources Sci. Technol. **10**, 595 (2001).
[23] E. W. Peterson and L. Talbot, AIAA J. **8**, 2215 (1970).
[24] M. C. M. van de Sanden, M. dan der Steen, G. J. H. Brussaard, M. Carrére, and D. C. Schram, Surf. Coat. Technol. **98**, 1416 (1998).
[25] M. A. Lieberman and A. J. Lichtenberg, *Principles of Plasma Discharges and Materials Processing* (Wiley, New York, 1994), p. 531.
[26] W. D. Davis and T. A. Vanderslice, Phys. Rev. **131**, 219 (1963).
[27] E. Stamate and H. Sugai, Phys. Rev. E **72**, 036407 (2005).